Chemical Geology 584 (2021) 120491

Contents lists available at ScienceDirect

Chemical Geology

journal homepage: www.elsevier.com/locate/chemgeo

Invited Research Article

Noble gas signatures constrain oil-field water as the carrier phase of hydrocarbons occurring in shallow aquifers in the San Joaquin Basin, USA

R. Karolytė [a,*], P.H. Barry [b], A.G. Hunt [c,e], J.T. Kulongoski [d], R.L. Tyne [a], T.A. Davis [d], M. T. Wright [d], P.B. McMahon [c], C.J. Ballentine [a]

[a] Dept. of Earth Sciences, University of Oxford, Oxford, UK
[b] Marine Chemistry & Geochemistry Dept., Woods Hole Oceanographic Institution, Woods Hole, MA, USA
[c] U.S. Geological Survey, Geology, Geophysics, Geochemistry Science Center, Denver, CO, USA
[d] U.S. Geological Survey, California Water Science Center, San Diego, CA, USA
[e] U.S. Geological Survey, Colorado Water Science Center, Denver, CO, USA

ARTICLE INFO

Editor: Don Porcelli

Keywords:
Noble gases
Hydrocarbons
Oil-field water
Reservoir
Multi-phase fluids
Isotope geochemistry

ABSTRACT

Noble gases record fluid interactions in multiphase subsurface environments through fractionation processes during fluid equilibration. Water in the presence of hydrocarbons at the subsurface acquires a distinct elemental signature due to the difference in solubility between these two fluids. We find the atmospheric noble gas signature in produced water is partially preserved after hydrocarbons production and water disposal to unlined ponds at the surface. This signature is distinct from meteoric water and can be used to trace oil-field water seepage into groundwater aquifers. We analyse groundwater ($n = 30$) and fluid disposal pond ($n = 2$) samples from areas overlying or adjacent to the Fruitvale, Lost Hills, and South Belridge Oil Fields in the San Joaquin Basin, California, USA. Methane (2.8×10^{-7} to 3×10^{-2} cm^3 STP/cm^3) was detected in 27 of 30 groundwater samples. Using atmospheric noble gas signatures, the presence of oil-field water was identified in 3 samples, which had equilibrated with thermogenic hydrocarbons in the reservoir. Two (of the three) samples also had a shallow microbial methane component, acquired when produced water was deposited in a disposal pond at the surface. An additional 6 samples contained benzene and toluene, indicative of interaction with oil-field water; however, the noble gas signatures of these samples are not anomalous. Based on low tritium and ^{14}C contents ($\leq$ 0.3 TU and 0.87–6.9 pcm, respectively), the source of oil-field water is likely deep, which could include both anthropogenic and natural processes. Incorporating noble gas analytical techniques into the groundwater monitoring programme allows us to 1) differentiate between thermogenic and microbial hydrocarbon gas sources in instances when methane isotope data are unavailable, 2) identify the carrier phase of oil-field constituents in the aquifer (gas, oil-field water, or a combination), and 3) differentiate between leakage from a surface source (disposal ponds) and from the hydrocarbon reservoir (either along natural or anthropogenic pathways such as faulty wells).

1. Introduction

Noble gases are non-reactive and act as conservative tracers where end-member compositions can be defined, thus providing bounds on the volume of differently sourced fluids that have contributed to any particular aquifer and/or crustal system (Ballentine et al., 2002; Ballentine et al., 1996; Ballentine et al., 1991). Terrestrial reservoirs (i.e., atmospheric, crustal, and mantle) have diagnostic noble gas isotopic signatures, and fluids derived from each reservoir can be discerned using noble gas analysis. For example, noble gas isotopic and abundance compositions from fluids in sedimentary basins have been used to successfully quantify physical exchange mechanisms between water, oil, and gas phases in conventional and unconventional hydrocarbon systems (Ballentine et al., 1996; Barry et al., 2018; Barry et al., 2016; Byrne et al., 2020; Byrne et al., 2018; Prinzhofer, 2013). Noble gases are also useful tracers of gases detected in groundwater, including mantle or crustal volatiles in cold or hydrothermal springs (Karolytė et al., 2019) as well as fugitive gases associated with hydrocarbon production

* Corresponding author.
E-mail address: ruta.karolyte@earth.ox.ac.uk (R. Karolytė).

https://doi.org/10.1016/j.chemgeo.2021.120491
Received 30 March 2021; Received in revised form 7 August 2021; Accepted 17 August 2021
Available online 18 August 2021

(Darrah et al., 2015; Darrah et al., 2014; Füri et al., 2009; Harkness et al., 2017; McIntosh et al., 2019). Further, noble gases can be used to differentiate between hydrocarbons sourced from the surface, depth, and potentially from enhanced oil recovery (EOR) practices (Barry et al., 2018), which are commonly used methods to improve hydrocarbon extraction efficiency. EOR is particularly prevalent in oil fields throughout California's San Joaquin Basin (SJB), where water resources are in high demand due to large agricultural and urban water consumption. The characterization of reservoir hydrocarbon fluids is critical for differentiating between natural and anthropogenically induced leakage into a groundwater system. The stark noble gas isotopic and abundance compositions contrast between surface and deep fluid sources allows for the differentiation of source fluids.

In this study, we use a novel geochemical approach to differentiate between hydrocarbons from reservoir, surface (produced and disposed), and microbial sources in the groundwater systems in parts of the SJB. This distinction is important, as it provides insight of the migration pathways and sources of hydrocarbon gases in aquifer systems, which are valuable natural resources, due to the sizable urban populations and agricultural activity in the vicinity (Mount and Hanak, 2014). A principal aim of the California State Water Resource Control Board's Oil and Gas Regional Monitoring Program is to define where there is evidence of oil and gas fluids in protected groundwater, thus providing information to resource management agencies about relative risks to groundwater (CSWRCB, 2019; USGS, 2020). Our approach utilises noble gas concentrations and isotope ratios in groundwater to understand the extent of exchange between hydrocarbons of different sources and aquifer systems.

Two companion studies explored geochemical, isotopic, and age dating (^{3}H, $^{3}He_{trit}$, SF_6 and ^{14}C) tracers to describe: (1) mechanisms for elevated radium activities and evidence for deep and shallow fluid mixing near these oil fields (McMahon et al., 2019) and (2) groundwater recharge patterns and limited detections of thermogenic gases in a high recharge setting overlying the Fruitvale Oil Field (Wright et al., 2019). They have identified the presence of oil-field water in three groundwater samples (out of 39) adjacent to a disposal pond in South Belridge Oil Field (McMahon et al., 2019), low concentrations of petroleum hydrocarbons in groundwater dominated by post-1950s recharge, and insufficient evidence for effects from production activities to the groundwater quality in the Fruitvale Oil Field area (Wright et al., 2019). Here, we focus on utilising the groundwater noble gas dataset in the subset of these samples to identify the specific physical processes (equilibrium exchange with hydrocarbons in gaseous or liquid phases), using the measured and modelled noble gas characteristics of the hydrocarbons in the area (Barry et al., 2018).

Thermogenic hydrocarbons are generated from thermocatalytic breakdown of organic material and their presence in shallow aquifers infers connectivity with hydrocarbon reservoirs at depth, while microbial hydrocarbons may be produced in shallow aquifers by microbial communities. These two types of hydrocarbons have distinct isotopic and gas wetness ratios (Etiope et al., 2009; Etiope and Sherwood Lollar, 2013); however, the isotope ratio data are only available for a subset of samples with substantial methane concentrations. Combining these standard techniques with noble gases, we are able to infer the hydrocarbon generation mechanism where hydrocarbon isotope data are unavailable, identify the carrier phase of the oil-field constituents in the aquifer (gas, oil, oil-field water, or a combination) and differentiate between possible leakage pathways (surface disposal ponds, leakage from reservoir/faulty wells, or natural geologic sources). The term 'oil-field water' refers to the formation water in the reservoir, which has interacted and equilibrated with hydrocarbons at depth.

2. Geological setting and samples

Water samples were collected from wells in Kern County, which is located in the southern region of the SJB (Fig. 1). The SJB is situated within the Central Valley of California, a ~ 700-km-long basin containing over 7500 m of Mesozoic through Cenozoic aged sediments (Scheirer and Magoon, 2007). Water samples with complete noble gas data used in this analysis were collected from 30 monitoring, public-supply, irrigation, and test wells located in the vicinity (within 5 km) of the three oil fields: Lost Hills, South Belridge and Fruitvale. Groundwater samples were collected from two groups of aquifers: overlying and adjacent to the oil fields (Table S1). Surface water samples were also collected from two produced oil-field water disposal ponds ($n = 2$, BSW) located at the southern edge of the South Belridge Oil Field. The Fruitvale Oil Field is located on the east side of the SJB. Water samples ($n = 12$, FGW) were collected from wells screened in intervals of unconsolidated to semi-consolidated gravel, sand, silt, and clay in Holocene and Pleistocene alluvium and older fluvial deposits in the Kern River Formation. Groundwater flow directions are generally from the east to the west/southwest (Wright et al., 2019). The South Belridge and Lost Hills Oil Fields are located on the west side of the SJB; sampled wells ($n = 7$, BGW and $n = 11$, LGW) are screened in unconsolidated to

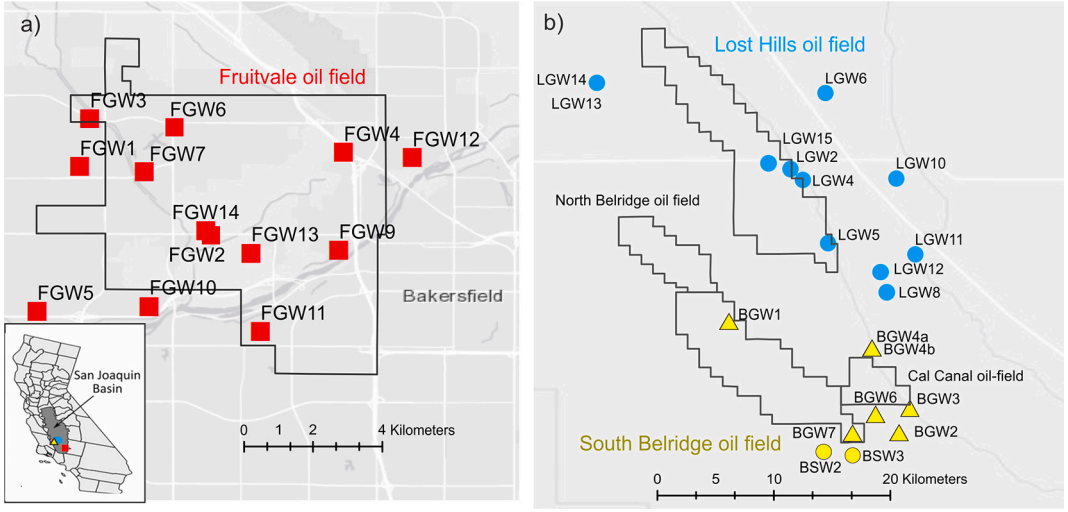

Fig. 1. Location maps of field boundaries and groundwater samples in Fruitvale (a), Lost Hills, and South Belridge (b) Oil Fields. Inset map shows the location of the oil fields (in respective colours) within the San Joaquin Basin. All markers represent groundwater samples with an exception of yellow circles which show produced water disposal ponds. (For interpretation of the references to colour in this figure legend, the reader is referred to the web version of this article.)

semi-consolidated sand, silt, and clay in Holocene/Pleistocene alluvium and fluvial, deltaic, to lacustrine deposits in the Tulare Formation. The aquifers are unconfined to semi-confined, except for water-bearing units in the Tulare Formation on the west side of the valley, which are confined by the Corcoran Clay Member of the Tulare Formation (Frink and Kues, 1954). Oil and gas producing zones in Fruitvale Oil Field include Santa Margarita, Chanac and the Etchegoin Formations (Miocene to Pliocene) (Hluza, 1965). In Lost Hills and South Belridge Oil Fields, hydrocarbons are produced from Oligocene to Pleistocene aged sediments of the Temblor, Monterey, Etchegoin, and Tulare Formations (California Department of Conservation, 1998; Scheirer and Magoon, 2007). Producing zones discussed in this paper include the Cahn zone in the Monterey Formation (Land, 1984), diatomite zones in the Monterey (Miocene) and Etchegoin (Pliocene) Formations, and the Tulare (Pleistocene) Formation (McMahon et al., 2018). Within Lost Hills and South Belridge Oil Fields, groundwater and oil wells are completed within the Tulare Formation. Hydrocarbon source rocks are within the underlying units (McLure Shale of the Monterey Formation and Rosendale Sandstone Member of Fruitvale Shale) (Magoon et al., 2009; Miller and Bloom, 1939). The median vertical separation between the top of oil well perforations and the base of freshwater is 100 and 130 m in South Belridge and Lost Hills Oil Fields, respectively (Davis et al., 2018a, 2018b), although inter-formational seal is provided by multiple layers of clays (Gillespie et al., 2019a, 2019b).

3. Methods

3.1. Sample collection and laboratory techniques

The sampling was conducted between 2014 and 2017 by the U.S. Geological Survey (USGS), in cooperation with the California State Water Resources Control Board (CSWRCB). Water samples were collected after purging three casing-volumes of water from the wells and included readings of pH, specific conductance, dissolved oxygen (O_2), and water temperature (Wilde, 2010). Water samples ($n = 32$) were collected in copper tubes (Hunt, 2015) and analysed for noble gas isotopes and abundances (Table S2) at the U.S. Geological Survey's Noble Gas Laboratory in Colorado, United States ($n = 30$, groundwater samples), and University of Oxford Noble Lab in the United Kingdon ($n = 2$, produced water from disposal pond samples (BSW2, BSW3)), following previously outlined operating procedures and analytical methods (Hunt, 2015; Tyne et al., 2019). Noble gas concentrations were reported at standard temperature and pressure (STP). Noble gas results were combined with tritium (^{3}H) concentrations, carbon-14 in dissolved inorganic carbon (^{14}C-DIC), concentrations of hydrocarbons CH_4 through toluene (C_1–C_7), and the isotopic composition of hydrogen and carbon in CH_4 (δ^2H-CH_4, δ^{13}C-CH_4), measured by USGS or contract laboratories. Descriptions of sampling methods and references for laboratory analytical methods for noble gases and the additional constituents are available in USGS data reports (Davis et al., 2018a, 2018b; Dillion et al., 2016; Gannon et al., 2018; Gillespie et al., 2019a, 2019b; McCarlson et al., 2018). A full list of laboratories responsible for individual measurements are listed in McCarlson et al. (2018).

3.2. Mudlog analysis

The mudlogs for oil and gas wells (CalGEM, 2020) within 500 m of collected groundwater samples ($n = 72$) in Lost Hills and South Belridge Oil Fields (Davis et al., 2018a) were analysed to evaluate if and where thermogenic gases were present in the groundwater aquifers overlying oil formations at the time of well drilling. The depth at which each hydrocarbon gas was first detected and depth of first oil show were recorded (Table S5). These records then were used to evaluate if hydrocarbon gases located in shallow groundwater were due to natural migration pathways prior to exploration activities.

3.3. Excess air modelling

Groundwater recharge temperature and the excess air component were determined by applying the unfractionated air (UA) (Ballentine and Hall, 1999) and closed-system equilibration (CE) (Aeschbach-Hertig et al., 2008) models, using inverse modelling software, PANGA (Jung and Aeschbach, 2018). Recharge salinity is assumed to be 0 mg/L for freshwater samples. Total dissolved solids (TDS) in disposal ponds were not directly measured; instead, they were estimated by adding all individually measured ions (27,957 and 13,562 mg/L for BSW2 and BSW3, respectively). ^{4}He concentrations and ^{3}He/^{4}He R/R_A, ratios (R is the ratio and R_A is the value of air (1.39×10^{-6}) were corrected for air bubble entrainment using the resolved ^{4}He excess air component (UA and CE models), giving (^4He_c) corrected values and ^{3}He/^{4}He R_c/R_A (subscript c denotes corrected ratio) (Kulongoski et al., 2013). The corrected concentrations and ratios therefore reflect the equilibrium atmospheric helium and terrigenic components. R_c/R_A was 1 when showing an atmospheric signature; lower values indicated presence of a crustal components (end-member $R/Ra = 0.02$) (O'Nions and Oxburgh, 1988) while higher values may indicate either mantle (end-member $R/R_a > 6$ (Graham, 2002)) or tritium addition.

3.4. Reconstruction of atmospheric noble gases in oil-field water

Pristine oil is free of atmospheric noble gases and acquire them through interaction with reservoir water. Consequently, oil-field water in the reservoir is expected to be depleted in noble gases relative to surface water. During production at the wellhead, the oil is depressurised and the volatile content of the oil ascends up the casing, while the produced fluids are pulled up the centre of the well (Tyne et al., 2019). The vast majority of volatiles are partitioned into the casing gases, which can be used to reconstruct the composition of oil within the reservoir (Ballentine et al., 1996). To reconstruct the atmospheric noble gas composition of oil-field water, we used the average reservoir conditions of the oil-bearing diatomite and Cahn zones and previously sampled casing gases from these zones (Barry et al., 2018). The diatomite zone is shallower (avg. sampled well depth 820 m) and more affected by EOR (water flooding), while the Cahn zone is deeper (avg. 1530 m) and preserves pristine signature unaffected by secondary fluid injection. These producing zones in the Lost Hills and South Belridge Oil Fields were chosen as end-members of heavily EOR-affected (diatomite) and pristine (Cahn) reservoirs. Given that the atmospheric noble gas concentrations in reservoir fluids are primarily controlled by the relative proportions of water, oil, and gas in the reservoir (Bosch and Mazor, 1988), the diatomite and Cahn zones provide bracketing end-member examples of reservoir hydrocarbons equilibrated with a high (diatomite) and low (Cahn) amount of water. Using the calculated reservoir temperatures (based on geothermal gradient, Table S6) and salinity conditions (Barry et al., 2018), we can calculate the expected noble gas composition of the oil-field water after equilibration with oil (Ballentine et al., 2002):

$$n^r_{ASW} = n^i_{ASW} - n_{oil} \quad (1)$$

$$n_{oil} = n^i_{ASW} \times \left(\frac{V_w \, \rho_w \, K_{oil}}{V_{oil} \, \rho_{oil} \, K_w} + 1 \right)^{-1} \quad (2)$$

where n is the number of moles (of individual noble gases), V is volume, superscripts r and i indicate remaining and initial water composition, $\rho$is density, Kw is Henry's Constant for water (Crovetto et al., 1982; Smith and Kennedy, 1983), and K_{oil} is Henry's Constant for oil. Reservoir salinity and reconstructed oil/water ratio (0.08 ± 0.05 and 0.3 ± 0.07 for diatomite and Cahn, respectively) were taken from Barry et al. (2018). Reservoir temperatures were calculated based on the average geothermal gradient (23 °C/km), which inferred from geophysical logs in Lost Hills and South Belridge Oil Fields (Gillespie et al., 2019a,

2019b). Henry's constants for oil were calculated based on reservoir American Petroleum Institute (API) gravity values, using linear interpolation between empirical measurements for a light oil (API of 34) and an heavy oil (API of 25) (Kharaka and Specht, 1988) for the sample-specific API values (Ballentine et al., 1996). The initial water composition (air saturated water (ASW) at 20 °C sea level and no salinity) was assumed to equilibrate with oil at Vo/Vw ratios defined above. The temperature of recharge is uncertain; however, the starting temperature variation had a negligible effect to the final results relative to Vo/Vw ratios. When Vo/Vw is infinitesimally small, the fractionation in the oil phase reaches its maximum. Conversely, when Vo/Vw - > ∞, oil phase obtains noble gas elemental ratios of ASW and the calculated oil-field water $^{20}Ne/^{36}Ar$ ratios are 0.33 ± 0.07 and 0.22 ± 0.06 for Cahn and diatomite, respectively. The error estimate included propagated uncertainty of reservoir temperature and Vo/Vw.

4. Results and discussion

4.1. The presence of hydrocarbons in the groundwater

Methane was detected in the majority of the groundwater samples (27 of 30), with concentrations ranging from 2.8×10^{-7} to 3×10^{-2} cm^3STP/g (Fig. 2). Trace amounts of C_2-C_7 (ethane to toluene) were detected in 14 groundwater samples and 2 oil-field water disposal ponds. In particular, BTEX group compounds (benzene and toluene) occurred in 7 groundwater samples, including BGW7 and LGW15 where benzene (15 and 9.79 μg/L, respectively) was above the maximum contaminant level (5 μg/L) defined by the U.S. Environmental Protection Agency (EPA) (EPA US, 2019). Full results of concentrations of CH_4 through toluene (C_1–C_7) and the isotopic composition of hydrogen and carbon in CH_4 (δ^2H-CH_4, $\delta^{13}C$-CH_4) are summarised in Table S1; however, stable isotope data exist only for a subset of the samples where methane concentrations were sufficiently high (> 2.5×10^{-4} cm^3STP/g). δ^2H-CH_4 and $\delta^{13}C$-CH_4 values fall off the theoretical mixing lines between a thermogenic and two microbial end-members (dashed lines, Fig. 3b), which can be explained by relative enrichment in $\delta^{13}C$ by methane oxidation (Whiticar, 1999) (Fig. 3b). Methane can be oxidised at a higher rate than higher molecular weight hydrocarbons (Whiticar, 1999), and therefore traditionally bacterial oxidation has been associated with decrease in C_1/C_{2+} ratios. However, when C_{2+} hydrocarbons constitute an already small proportion of the total hydrocarbon budget, the depletion of their relative smaller pool has been shown to lead to an inverse trend of C_1/C_{2+} ratio increase (Martini et al., 2003; Martini et al., 1998; Martini et al., 1996) (Fig. 3b). The rapid biodegradation of C_{2+} hydrocarbons in oxygen-rich aquifers, which occurs in parts of the study area (McMahon et al., 2019), precludes using hydrocarbon concentration data to evaluate the total volumes of reservoir-fluids in the water. We further investigated hydrocarbon sources and transport mechanisms through noble gas signatures of the groundwater.

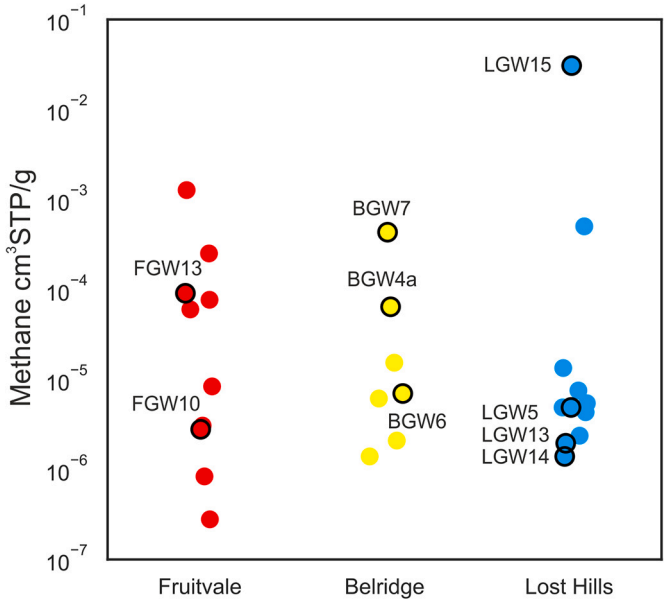

Fig. 2. Methane concentrations in aquifers adjacent and overlying the oil fields. Symbols with black outlines indicate samples where trace amounts of benzene and/or toluene were detected.

4.2. Investigating the interaction with reservoir fluids using atmospheric noble gases

The concentration of atmospherically derived noble gases (^{20}Ne, ^{36}Ar, ^{84}Kr, ^{132}Xe) in groundwater are primarily controlled by equilibration with air at a given temperature, atmospheric pressure, salinity, and accounting for excess air components from bubble entrainment (Ballentine and Hall, 1999; Stute and Deak, 1989). Noble gas isotopic and elemental abundances are reported in Table S2. The physical conditions during the addition of excess air, such as pressure and the relative volume change in entrapped air bubbles, lead to different elemental fractionation from the air signatures in the excess component (Aeschbach-Hertig et al., 2008; Jung and Aeschbach, 2018). The equilibrium and excess air values defined by recharge conditions may be further overprinted by interaction with oil or hydrocarbon gas. Here, we investigated the atmospheric noble gas change in ASW as a result of three different processes: 1) addition of excess air, 2) equilibration with a migrating gas phase (gas stripping), and 3) mixing with modelled oil-field water (calculated concentrations in oil based on Henry's K in Table S3). Fig. 4 shows the freshwater ASW composition range of 10–40 °C with the modelled fractionation curves on $^{20}Ne/^{36}Ar$ vs ^{132}Xe, ^{84}Kr, ^{36}Ar, and ^{20}Ne (calculated based on Ballentine et al., 2002) plots using ASW at 15 °C as a starting point. Interaction with hydrocarbons (both oil and gas phases) leads to elemental groundwater depletion in noble gases, whereas the addition of excess air leads to elemental enrichment, while the isotopic ratios are unaffected. Groundwater that has been in contact with oil is most easily identified with increasing concentrations of the heavier noble gases (Kr, Xe) due to their higher solubility. Fig. 4 shows that the majority of South Belridge and Lost Hills Oil Field samples can be explained by simple equilibration in the temperature range of 14–19 °C, with moderate addition of excess air (solid black line), while the majority of Fruitvale Oil Field samples showed a much more significant excess air component. Three groundwater samples fall on the mixing line with noble-gas-depleted oil-field water (BGW4a, BGW7, LGW15, blue line); however, BGW4a has a significant excess air component and its final composition is affected by both of these vectors. We will discuss the interaction of hydrocarbons in a gas phase, the oil-field water, and excess air addition separately in the following sections.

4.2.1. Gas stripping

During the equilibration between gas and water, noble gases elements are preferentially partitioned into the gas phase according to Henry's Law. Partitioning may occur when stray methane migrates through the water in volumes larger than the water solubility limit under the temperature and pressure conditions of the aquifer and has been previously identified in aquifers overlying hydrocarbon-rich formations (Darrah et al., 2015; Darrah et al., 2014; Wen et al., 2017; Wen et al., 2016). The remaining water (Eq. 3) phase becomes preferentially depleted in lighter noble gases relative to the heavy noble gases, such that all noble gas concentrations negatively correlates with $^{20}Ne/^{36}Ar$ values.

$$n_{asw} = n^i_{asw}\left(\frac{V_g}{V_w}K_w + 1\right)^{-1} \quad (3)$$

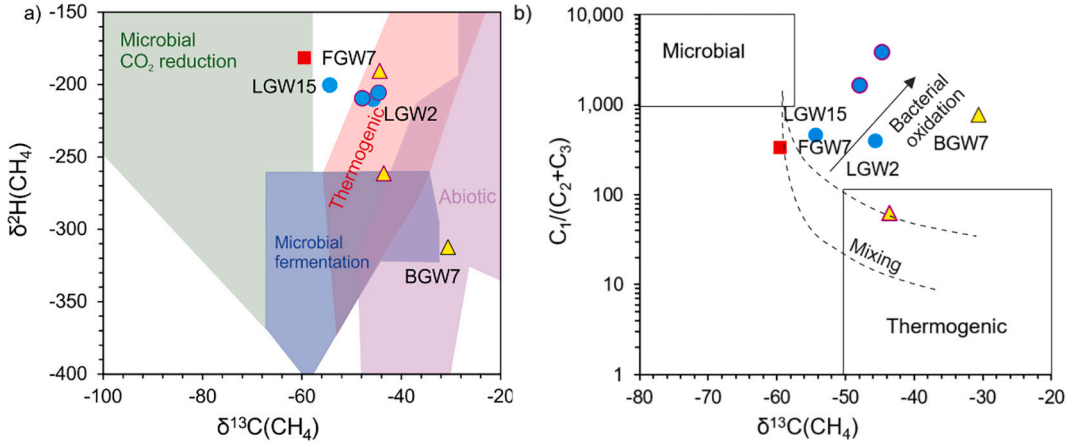

Fig. 3. a) $\delta^{13}C(CH_4)$ vs $\delta^{2}H(CH_4)$ diagram showing empirically observed source signatures (Etiope and Sherwood Lollar, 2013) b) Bernard plot showing typical microbial and thermogenic methane compositions (Etiope et al., 2009). Samples shifted off the calculated mixing lines between a microbial and two thermogenic end-members (theoretical) by bacterial aerobic oxidation (Whiticar, 1999). Purple outlines indicate samples for which no noble gas data are available, displayed for reference.

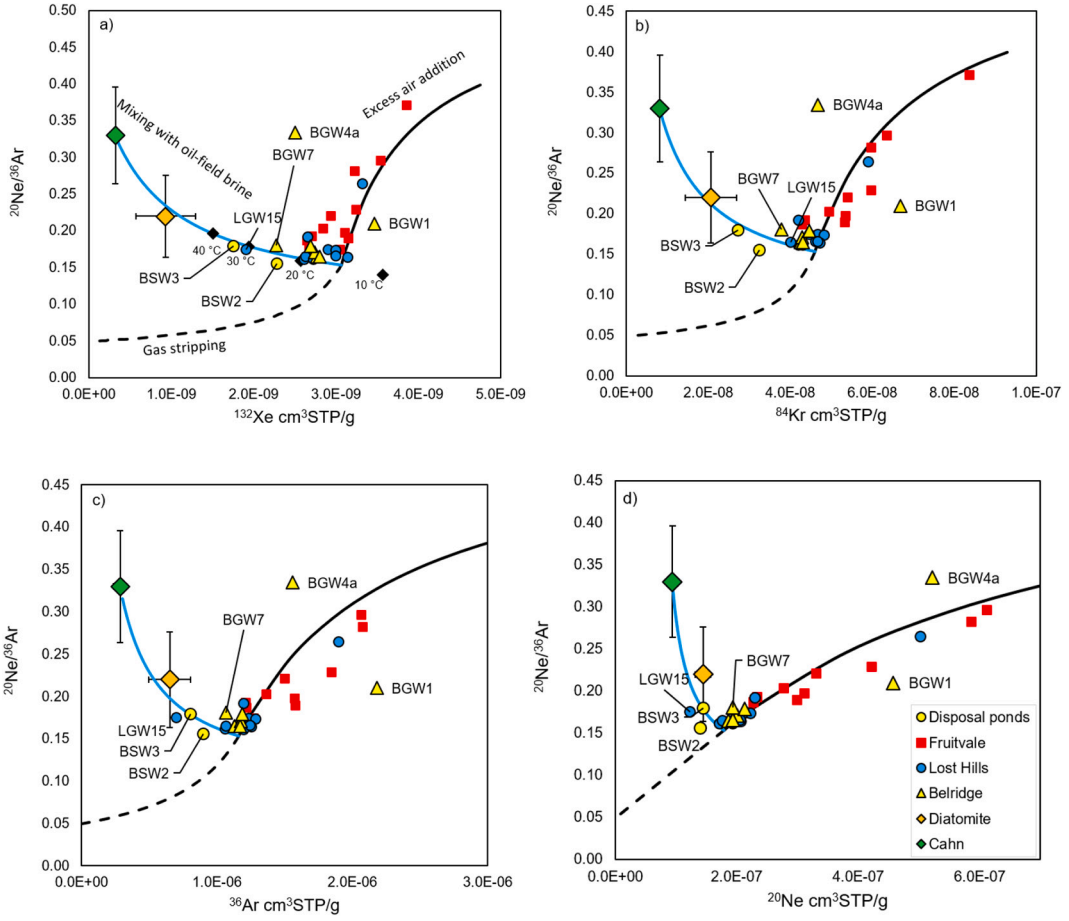

Fig. 4. a) $^{20}Ne/^{36}Ar$ vs ^{132}Xe plot showing ASW at 15 °C (intersection of three curves) and water evolution trajectories for addition of excess air (solid), gas stripping (dashed) and mixing with reservoir water (blue). The excess air line is displayed for reference using the UA (unfractionated air) model; however, a mixture of CE (closed system equilibrium) and UA models were best fit to the samples. The green and orange diamonds show reconstructed compositions of Cahn and diatomite oil-field water (Lost Hills Oil Field). Black diamonds (Fig. a) show ASW for the temperature range 10–40 °C. The majority of the samples can be explained by equilibration with the atmosphere at 14–19 °C with addition of excess air, which is especially high for Fruitvale Oil Field samples. Five outlier samples (BSW2, BSW3, BGW4a, BGW7 and LGW15) fall on the mixing line with reservoir water. Importantly, these trends are consistent within all atmospheric noble gases ($^{20}Ne/^{36}Ar$ vs ^{132}Xe (a), ^{84}Kr (b), ^{36}Ar (c) and ^{20}Ne (d) space). (For interpretation of the references to colour in this figure legend, the reader is referred to the web version of this article.)

None of the data from this study fall on the modelled gas stripping line (black dashed line, Fig. 4). The minimum gas/water volume ratio required to equilibrate to produce fractionation in the range observed within the fitted UA and CE excess air models is 0.002, which would deplete the water ^{20}Ne concentrations by 15% and decrease the $^{20}Ne/^{36}Ar$ value of the groundwater by approximately 0.02. For instance, The ASW end-member at 15 °C ($^{20}Ne/^{36}Ar = 0.15$) when undergoing a 15% decrease in ^{20}Ne would have a $^{20}Ne/^{36}Ar$ ratio of 0.13. Hydrocarbon gas migration through the aquifer in volumes larger than 0.2% of the total aquifer volume and at significantly higher rates than the aquifer water flow can therefore be ruled out. Any stray gas migrating through the groundwater can therefore be assumed to fully dissolve in the water.

4.2.2. Mixing with oil-field water

In contrast to gas stripping, this equilibration with oil preferentially removes heavy noble gases and leads to increasing $^{20}Ne/^{36}Ar$ in the water, coupled with a decrease in noble gas concentrations.

Oil-field water is often expected to have elevated TDS, volatile organic compounds, and higher concentrations of hydrocarbon compounds (specifically $C_1/C_{2+} < 100$ and δ13C-CH4 < -50‰). Oil-field water can include a mixture or hydrocarbon reservoir formation fluids and water injected for enhanced recovery. The reconstructed oil-field water (Table S3) is depleted in atmospheric noble gases relative to ASW (Fig. 4). The mixing line between average ASW composition and oil-field water overlaps with the values expected from groundwater recharge at increasing temperatures (shown as black diamonds on Fig. 4a) and therefore could be attributed to a recharge temperature anomaly. The average recharge temperatures of groundwater within the Tulare Formation, reconstructed using excess air modelling, are 18.4 ± 3.8 °C and 18.6 ± 3.1 °C in South Belridge and Lost Hills Oil Fields, respectively (Table S4). Five samples (BSW2, BSW3, BGW4a, BGW7 and LGW15) are outliers from the main sample group and fall between the ASW and reconstructed oil-field water end-members. BSW2 and BSW3 are unlined produced water disposal ponds, which represent the composition of oil-field waters, potentially mixed from multiple sources, and partially re-equilibrated with the atmosphere at the surface. BGW4a additionally has a high excess air component and is therefore shifted by both of these vectors. Typically, produced reservoir fluids are treated to separate the hydrocarbons from the brine at dehydration plants. The separation may include a combination of chemical treatment (emulsion breakers) and floatation cells. The dehydration process is isolated from the atmosphere, so no re-equilibration with the atmospheric component is expected. Produced brine further re-equilibrates after disposal to the pond, but this is restricted to the top water layer at the interface with the atmosphere and is unlikely to be sufficient for complete re-equilibration. The exact protocol and timing of produced brine treatment and the length of time since disposal to the pond in BSW2 and BSW3 are unknown. The noble gas composition of the disposal pond samples can be interpreted using two alternative scenarios: 1) pond samples preserve the original signature acquired by initial freshwater recharge, followed by equilibration with oil (diatomite, produced in the South Belridge Oil Field) and subsequently partially re-equilibrated with ambient atmosphere; 2) pond samples have completely re-equilibrated with the ambient atmosphere at the disposal pond and the observed noble gas signature represents brine salinity, temperature, and pressure conditions of the pond environment. Considering that the complete re-equilibration typically requires significant gas flow, water mixing, and atmospheric exposure, we believe that the most likely interpretation is a combination of both. However, even if the second scenario is dominant, this does not preclude using the distinct noble gas composition of disposal ponds as an end-member where leakage from a surface source is suspected.

The remaining three outliers, BGW4a (monitoring well), BGW7 (irrigation well), and LGW15 (oil-field water supply well), are groundwater samples from the Tulare Formation and/or the overlying alluvium. The apparent recharge temperatures in these samples are 30, 29, and 34 °C, respectively, which are significantly higher than the average recharge temperature in the aquifer (18 °C). The methane contents are moderate in BGW4a and BGW7 (4.3×10^{-4} and 6.4×10^{-5} cm^3/g) and at water saturation limit in LGW15 (3.1×10^{-2} m^3/g). These wells contain other evidence of interaction with oil, hydrocarbon gas, and or oil-field water. Benzene was detected in all three wells and toluene in two of the wells (Table S1). Benzene concentrations were above the Maximum Contaminant Level (5 μg/L) defined by the U.S. Environmental Protection Agency (EPA) (EPA, 2019) in BGW7 (15.1 μg/L) and LGW15 (9.79 μg/L). These three wells had the TDS values (5590 to 15,900 mg/L) significantly elevated to median TDS in South Belridge and Lost Hills Oil Fields (4280 and 2400 mg/L, respectively). LGW15 contains trace amounts of other dissolved hydrocarbon gases, including ethane, propane, butane, and isopentane consistent with a thermogenic source (Gilman et al., 2013). The combined evidence from multiple geochemical indicators suggest groundwater mixing with oil-field water in these three samples. The observed depletion in atmospheric noble gas concentrations indicates that the carrier phase of these hydrocarbon compounds is primarily oil-field water, migrating separately from the oil phase with hydrocarbons in it. Microbial oxidation trend observed in the CH_4 isotopic and gas wetness signatures (Fig. 3) indicates that hydrocarbons were affected by biodegradation, and therefore the detected concentrations are a minimum estimate. Importantly, the oil-field water signature associated with depletion in noble gas concentrations and increase in $^{20}Ne/^{36}Ar$ ratios is reported here for the first time, and is distinct from previous studies, which reported negative correlation between $^{20}Ne/^{36}Ar$ ratios and ^{20}Ne concentrations due to interaction with a gas phase (Darrah et al., 2015; Wen et al., 2016). The possible pathways include leakage of produced fluids after separation from the oil phase at the surface, from surface infrastructure or disposal pond facilities, or migration from depth through fractures, natural or induced, faulty well casing, or natural water flowpaths and faults (Darrah et al., 2014; Dusseault and Jackson, 2014). The analysis of mudlogs located within 500 m of groundwater samples overlying the fields revealed some instances where trace amounts of oil and gas were detected above the producing reservoir, including one well with natural C_1-C_3 hydrocarbon gas shows as shallow as 270–340 m depth within 500 m of BGW7 (Table S5) (CalGEM, 2020), although oil and gas shows in other mudlogs were deeper. However, the sampled South Belridge Oil Field water well depths are shallower (91–192 m; BGW7 75–165 m) and generally lack evidence of mixing with oil-field water; therefore, widespread natural aquifer and oil-field connectivity is unlikely. Multiple historical and some active (to 2018) disposal ponds exist in the vicinity of BGW7 and BGW4a (), including BSW2, located 2.4 km up the topographic gradient from BGW7 (CalGEM, 2020). These ponds are the likely surface source of oil-field water. BGW4a, completed in the alluvium, contains a high excess air component (224% ΔNe) relative to closely located BGW4b (12% ΔNe), completed in the underlying Tulare Formation. The excess air component is therefore likely associated with the oil-field water, which recharges to the water table from a surface source (ponds), affecting the shallower alluvium. The excess air component in BGW7 is lower (21% ΔNe); however, helium and microbial methane evidence is consistent with a surface source (discussed further in Section 4.3.1). In contrast, mixing with non-degassed oil-field water from a subsurface source is more likely in LGW15, due to the low excess air component (unresolvable) and high methane concentrations (0.03 cm^3STP/g). There are 424 oil and gas wells, 247 of which are plugged or buried in the 500 m radius around LGW15 and 1 disposal pond (within 600 m distance) (Fig. S2) (CalGEM, 2020). The median vertical separation between the petroleum-bearing members of the Tulare Formation and overlying aquifers is low (130 m) (Davis et al., 2018a, 2018b) and oil shows are noted in mudlogs starting from 230 m below surface (Table S5); therefore, natural brine migration cannot be excluded, although it would require a geological explanation for oil-equilibrated brine separation from the oil phase prior to the ascent to the aquifer.

A broad range of geochemical indicators for oil-field water mixing

with groundwater in the Lost Hills/South Belridge Oil Field study area was previously reported (McMahon et al., 2019); oil-field water in BGW7 and BGW4a was identified based on high radium activities, elevated Cl, Br, Li contents, and enriched $\delta^2H(H_2O)$ and $\delta\ ^{18}O(H_2O)$. LGW15 was not discussed in this study, because they focused on samples with high radium activities, but is reconsidered here because of the noble gas depletion, C_1-C_7 hydrocarbons, and elevated TDS.

Based on the atmospheric noble gas depletion trend (Fig. 4), the calculated fraction of oil-field water is 0.3 ± 0.1 BGW7, 0.6 ± 0.2 in BGW4a and 0.6 ± 0.2 in LGW15. The uncertainty associated with oil/water ratio in the reservoir and initial water recharge temperature is reflected in the uncertainties. The calculated oil-field water fraction is in strong agreement with the independent estimates reported above (0.4 in BGW4a and BGW7) (McMahon et al., 2019) and increases our confidence in the validity of the method. The sampled water wells are not potable; however, these findings have implications for safe water use especially in old groundwater where aquifer recharge and flushing of contaminants is slow.

BTEX compounds (benzene and toluene) below the maximum contaminant level were detected in 6 other groundwater samples (Table S1), where anomalous noble gas signatures were not detected. BTEX occur naturally in hydrocarbon reservoirs and are highly soluble in water (Njobuenwu et al., 2005). The presence of BTEX in groundwater may be associated with surface spills of produced fluids (Gross et al., 2013; Shores et al., 2017) or oil-field water migration from depth due to natural upward migration of oil-field water in close vertical proximity to groundwater or leaky wells (McMahon et al., 2017). Samples with BTEX components in South Belridge and Lost Hills Oil Fields have low tritium (below detection limit to 0.3 TU) and ^{14}C (0.87–6.9 pcm) contents, which are also lower than average values in samples without BTEX. BTEX may therefore be associated with deep fluid migration rather than surface spills (Landon and Belitz, 2012). However, both natural and anthropogenic sources are possible and may include leaky wells or natural fault zones.

4.2.3. *Tracing enhanced recharge in Fruitvale Oil Field*

The majority of the Lost Hills and South Belridge Oil Field samples (n = 10, n = 5, respectively, excluding those discussed above) cluster around the ASW values at recharge temperatures between 14 and 19 °C and can be explained by simple equilibration with addition of moderate excess air component (Fig. 4). The observed Ne excesses in Fruitvale Oil Field samples (up to 824% ΔNe (FGW10), mean 163% ΔNe) (Table S4) are a factor of ten higher than reported from natural recharge conditions (Kipfer et al., 2002). The CE excess air model (best fit for Fruitvale Oil Field samples) describes only partial dissolution of entrapped air bubbles, which means that the total fraction of entrapped air in the aquifer is even higher than what is observed is solution.

A high excess air component is systematically observed in areas with active enhanced recharge programs characterised by rapid infiltration (Heilweil et al., 2004), which often utilise surface recharge ponds to replenish the aquifers. Median Ne concentration in areas impacted by enhanced recharge are found to be 50% higher than those characterised by natural recharge (Cey et al., 2008). Median Ne concentrations in Fruitvale Oil Field samples are 54% higher than in Lost Hills and South Belridge Oil Fields, in line with observations outlined above (Cey et al., 2008). The Kern River is a major source of recharge in the area (Faunt, 2009). During the last few decades, the recharge from the Kern River has been enhanced with water spreading facilities, located along the riverbanks in the Fruitvale Oil Field study area (Kern County Water Agency, 2018). ^{20}Ne excess is significantly correlated with the amount of tritium in the water (p = 0.02) (Fig. 5a) and the distance to the Kern River (p = 0.007), indicating that large ^{20}Ne excesses are linked to recent enhanced recharge from the banks of the Kern River (Fig. 5b).

Oil production in the Fruitvale Oil Field relies upon injection of large amounts of recycled produced water into target formations for enhanced recovery and water disposal. The injectate fluids have been characterised to have an air-like atmospheric noble gas ratios (Barry et al., 2018) and, in the event of mixing of oil-field fluids with groundwater, could be expected to add large amounts of air-like noble gases to the groundwater. However, the majority of groundwater samples with noble gas data are located more than 1 km from active injection wells, are much shallower (median depth 210 m) than the injection depths (median depth 1315 m) (CalGEM, 2020), and the wells in the vicinity of injection wells are not characterised by the highest Ne excesses. The unusually high excess air components therefore indicative of enhanced recharge in the Fruitvale Oil Field area. This interpretation is in agreement with results from a companion study, which reported primarily post-1950s recharge in the Fruitvale Oil Field aquifers (Wright et al., 2019). Excess Ne correlates with ^3H concentrations, suggesting the highest modern groundwater input is related to the practices of riverbank spreading. The rapid recharge means that the aquifer residence time is low, and if any oil-field water or thermogenic methane does reach groundwater, it would be difficult to detect via groundwater monitoring.

4.3. *^4He sources*

Helium isotopes (Rc/R_A) in Fruitvale Oil Field samples (n = 12) span from 0.43 to 2.61 (where R_A is the value of air (1.39×10^{-6}), and Rc denotes ratio corrected for excess air contribution. South Belridge Oil

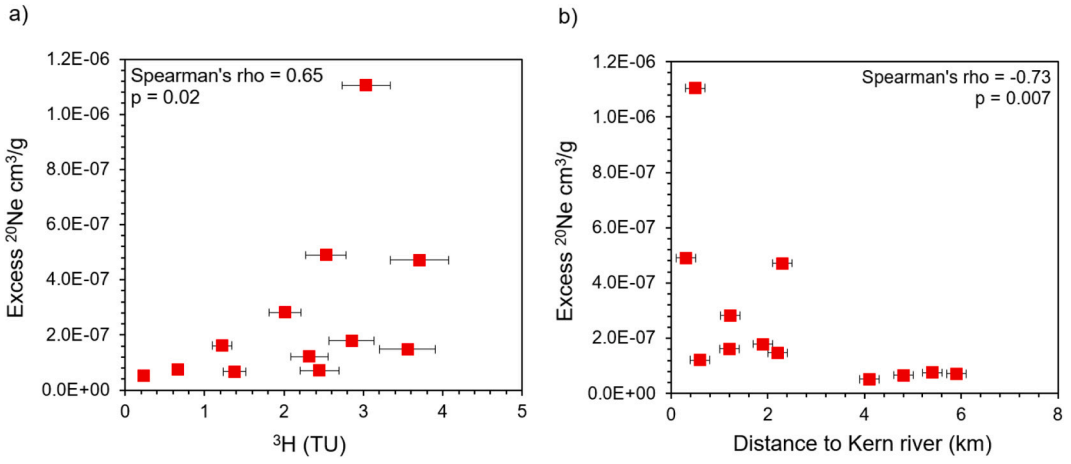

Fig. 5. Resolved excess ^{20}Ne concentrations (CE model) positively correlate with ^3H contents in Fruitvale Oil Field samples (a). ^{20}Ne excesses decrease with increasing distance from the Kern River (b).

Field Rc/R_A values range from 0.23 to 0.98 and 0.67–0.7 in groundwater samples ($n = 8$) and oil-field water disposal ponds ($n = 2$); Lost Hills Oil Field ($n = 11$) values range from 0.05 to 0.46 and correspond to the highest He concentrations (up to 1.14×10^{-6} $cm^3STP/cm3$). The groundwater samples fall into two distinct groups (Fig. 6). In the first group, consisting of the majority of Fruitvale Oil Field samples, ^4He concentrations increase with ^{20}Ne at a constant $^4He/^{20}Ne$ ratio of 0.31 (Fig. 6a), equal to that of air (Ozima and Podosek, 2002). This suggests that nearly all ^4He above ASW equilibrium levels in these samples is sourced from the atmospheric excess air component, in line with excess air addition discussed in section 4.3.3. In the second group of samples, including one Fruitvale Oil Field sample (FGW7) and most groundwater samples from Lost Hills and South Belridge Oil Fields (all except LGW8, BGW1, BGW4a), the increase in ^4He is not correlated with ^{20}Ne, suggesting the majority of ^4He is not added by an atmospheric excess air solubility-controlled process (Fig. 6a). In the first group, $^3He/^4He$ values of most of these samples are 1 R_A or higher, indicating addition of tritogenic ^3He and no significant radiogenic ^4He component (Fig. 6b). In contrast, in the second group $^3He/^4He$ values are all below the atmospheric value of 1 R/R_A and track with decreasing $^{20}Ne/^4He$ (Fig. 6b). This group of samples has a significant non-atmospheric ^4He component, which could be sourced from hydrocarbon fluids, either from a reservoir or a shallow (post-production) source, or natural radiogenic ^4He accumulation in groundwater with long residence times.

4.3.1. *Investigating the link between radiogenic ^4He and CH_4*

To assess if the radiogenic helium isotope ratios in groundwater ($^3He/^4He < 1$ Rc/R_A) are linked to the presence of hydrocarbons, we consider three potential carrier phases of thermogenic methane in groundwater: methane dissolved in non-degassed crude oil (reservoir oil), methane as a pure gas phase (reservoir CH_4), and methane dissolved in oil-field water (reservoir H_2O). We use ^4He concentrations in casing gas samples from 8 oil production wells in Cahn and diatomite zones within the Lost Hills Oil Field (Barry et al., 2018) to reconstruct average ^4He concentrations expected in oil-field water and non-degassed reservoir oil, using the method outlined in Barry et al. (2018). The reconstructed mean ^4He concentrations in reservoir oils are $7.4 \pm 6 \times 10^{-4}$ cm^3STP/g. The lower end of the range reflects hydrocarbons affected by EOR injection; the higher end represents oil where injection did not occur. Lastly, we calculate the expected ^4He concentrations in oil-field water after equilibration with oil, assuming that ^4He concentrations are controlled by equilibration with the oil phase ($1.3 \pm 1.4 \times 10^{-7}$ cm^3/g), using Eq. 2 in Section 3.3. The full results for average casing gases, non-degassed reservoir oil and oil-field water are summarised in Table S6.

Based on the lack of evidence for gas stripping by free-phase gases in the aquifer discussed in Section 4.2.1, we can assume that all thermogenic methane added to the water dissolves. We can therefore describe the interaction between ASW and thermogenic hydrocarbon gas sources as simple mixing for all three end-members (reservoir H_2O, reservoir CH_4, reservoir oil in Fig. 7). The solubility limit for methane dissolution into water at 20 °C is 0.034 cm^3/g (shown as dashed horizontal line in Fig. 7).

Fig. 7 shows the mixing between three reconstructed end-members and ASW at 20 °C in a ^4He versus CH_4 plot. The mixing between ASW

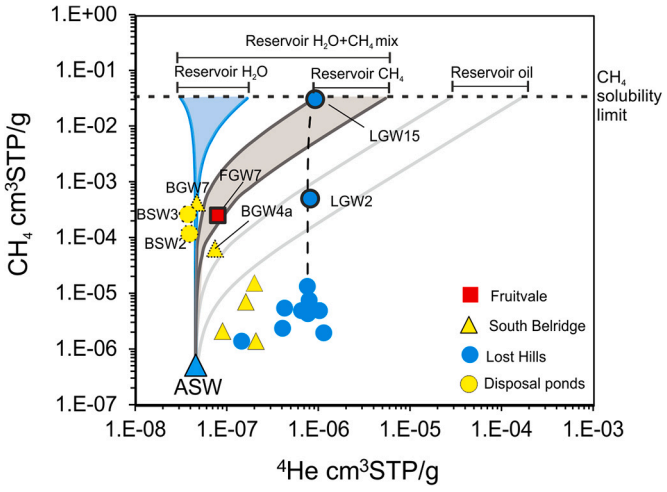

Fig. 7. CH_4 vs ^4He_c concentrations including only the samples with $^3He/^4He$ ratios <1 Rc/R_A ($n = 20$). Methane solubility limit (0.034 cm^3/g at 20 °C, 1 atm) represents the maximum amount of methane that can be added within the framework of a simple mixing model (horizontal dashed line). The reconstructed reservoir water, gas, and oil values are shown at the top. The blue area represents the mixing space with reservoir water, the grey area shows mixing with reservoir gas, and white area shows mixing with oil. Samples in the combined space of these areas could be mixing with a combination of these end-members. Dashed vertical line shows mixing between mean Lost Hills Oil Field samples and reservoir CH_4 end-member. The outlines of symbols indicate additional evidence for thermogenic gas source: dotted – C_2+ hydrocarbons, thick solid line – C_2-C_7 hydrocarbons, and thermogenic methane isotope ratios. (For interpretation of the references to colour in this figure legend, the reader is referred to the web version of this article.)

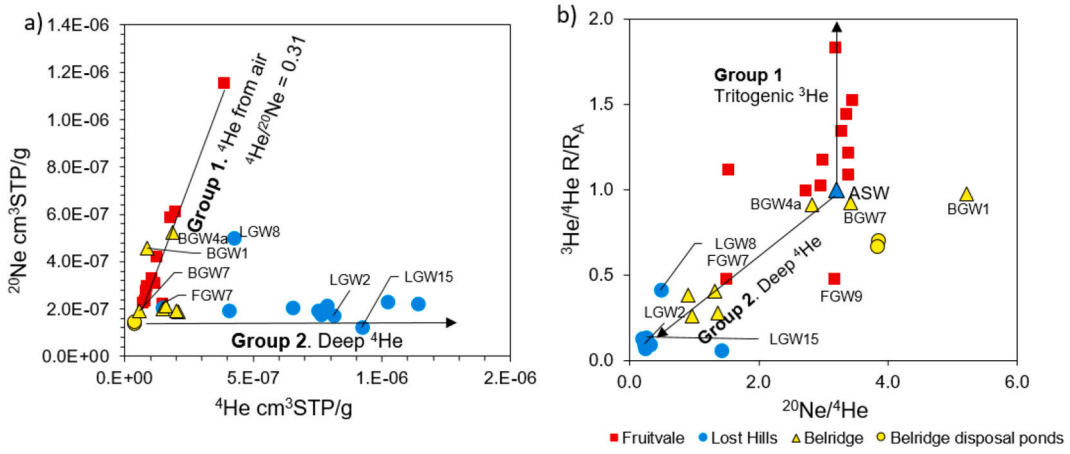

Fig. 6. He—Ne system of the groundwater samples. The samples are in two distinct groups: the first group shows a positive correlation between ^4He and ^{20}Ne concentrations at a constant ratio of 0.31 (a) and $^3He/^4He$ values above atmospheric ratio of 1 R/R_A without a change in $^{20}Ne/^4He$ ratios (b), indicating all ^4He is sourced from excess air rather than a deep source. The second group of samples is characterised by decoupled ^4He and ^{20}Ne concentrations (a), $^3He/^4He < 1$ R_c/R_A, and decreasing $^{20}Ne/^4He$ ratio (b). There is a significant deep ^4He component in this group of samples.

and oil-field water (reservoir H_2O), which is depleted in noble gases relative to ASW (Table S3), yet has a radiogenic $^3He/^4He$ signature and can be saturated with thermogenic methane, is not expected to produce significant isotopic enrichment in ^4He. Two groundwater samples fall on this trend (BGW4a, BGW7) and disposal pond samples (BSW2, BSW3), showing ^4He depletion and increased methane concentrations relative to the other four South Belridge Oil Field samples. This observation is consistent with presence of oil-field water identified in BGW4a and BGW7 by atmospheric noble gases. Methane stable isotopes in BGW7 indicate microbial fermentation, followed by enrichment of the $\delta^{13}C$ (CH_4) values by oxidation (Fig. 2). Methane is likely sourced from shallow fermentation of organic carbon in water derived from the oil-field water disposal ponds.

In Fruitvale Oil Field, only two samples indicate the presence of non-atmospheric ^4He (FGW7, FGW9, $^3He/^4He$ = 0.43 and 0.48 Rc/R_A, respectively). FGW7 falls in the mixing zone with reservoir gas, while FGW9 does not contain methane. Stable isotope data indicate mixing between thermogenic and microbial methane (Fig. 3) and a trace amount of ethane in FGW7, while TDS, major ion, and radium concentrations in both samples are consistent with the rest of the Fruitvale Oil Field group of samples. Given the previously discussed fast freshwater recharge in Fruitvale Oil Field, it is unlikely that elevated ^4He contents are produced in-situ. ^4He is likely introduced by thermogenic methane in a gas phase migrating from the reservoir, either through natural flow paths or associated with oil production activities. Some thermogenic methane may be present in FGW7, but the absence of methane in FGW9 in association with non-atmospheric ^4He may indicate methane has been microbially consumed.

The majority of Lost Hills and three South Belridge Oil Field samples cluster at relatively low methane concentrations ($< 1.1 \times 10^{-5}$ cm^3STP/g) and high ^4He contents ($1 \times 10^{-7} > cm^3STP/g$). These samples do not fall on the mixing lines with any reconstructed end-members. The median $^4He/CH_4$ ratio in these samples is 0.13, which is much higher than expected even in crude oil ($\sim 3 \times 10^{-4}$, Fig. 7). It is therefore most likely that ^4He and methane concentrations in these samples are decoupled and represent natural radiogenic ^4He accumulation in the aquifer during a long water residence time and, most likely, microbial methane source. LGW2 and LGW15 are outliers from this group with significantly higher methane contents. Thermogenic methane is likely transported to LGW15 in solution in oil-field water, identified in Section 4.3.2; no evidence for oil-field water in LGW2 suggests a possible migration in a gas phase.

The combination of stable isotopes, radiogenic and atmospheric noble gases allows us to distinguish between the migration of non-degassed oil-field water from the reservoir (LGW15) (no significant depletion in ^4He contents, atmospheric noble gas depletion, thermogenic CH_4 signature) and leakage from degassed oil-field water in disposal ponds (BGW4a, BGW7) (depletion in both ^4He and atmospheric noble gases relative to background in the aquifer, microbial methane oxidation signature after exposure at the surface) as carrier phases of hydrocarbon compounds into the water.

4.4. Implications for the use of noble gases as tracers in hydrocarbon tracing studies

The noble gas isotopic composition of oil-field water is expected to reflect radiogenic values (Rc/R_A – 0.02); however, the overall noble gas concentrations are expected to be lower than ASW due to equilibration with the oil phase. Consequently, the crustal isotopic signature of oil-field water can be easily overprinted by mixing with ASW. The $^3He/^4He$ ratio in samples where oil-field water has been identified ranges from 0.90 to 0.91 Rc/R_A, only slightly lower than the atmospheric value and higher than the naturally ^4He-rich waters in Lost Hills Oil Field (0.05–0.37 Rc/R_A) due to long residence time (Fig. 7). The use of ^4He as an indicator for deep fluid excursion can therefore be limited in groundwaters where high ^4He contents are present due to long residence times, or when the brine is noble gas depleted. The elemental fractionation in the atmospheric noble gas component caused by interaction with liquid or gaseous hydrocarbons preserves crucial information about phase interaction and should be used in conjunction to assess the evidence for physical equilibration processes. The atmospheric noble gas signatures allow us to constrain the fluid movement and differentiate between oil-field water mixing with groundwater by recharge from surface disposal ponds (degassed and/or high excess air) and reservoir (non-degassed, low excess air) as well as trace enhanced groundwater recharge (high excess air). The rapid biodegradation of C_{2+} hydrocarbons in oxygen-rich aquifers precludes using hydrocarbon concentration data to evaluate the total volumes of reservoir-fluids in the water and may mask the signals for connectivity between reservoir-fluid bearing components and groundwater, while isotopic signatures in hydrocarbon compounds are often below the detection limit at low gas concentrations. Given these limitations of the standard techniques, clear benefits exist in including noble gas analysis in the standard analytical procedure of investigating potential hydrocarbon gas sources in groundwater. Noble gas analyses are the most beneficial in instances where sources are hard to identify due to hydrocarbon to degradation of hydrocarbon compounds (for instance, historical leaks) or tracing produced water, where these compounds are present in small amounts. Due to relatively higher costs compared to standard hydrocarbon gas and isotopic analysis, noble gases may be the most useful in investigative cases rather than routine monitoring.

5. Summary

Here for the first time we show that atmospheric noble gas depletion associated with interaction with an oil phase provides a distinctive noble gas depletion signature to oil-field water, which can be used to trace its presence in groundwater aquifers. We identify oil-field water in three groundwater samples (LGW15, BGW4a and BGW7) and are able to discern between oil-field water migration after production from disposal ponds and from the subsurface reservoir. Trace amounts of benzene and toluene were identified in 6 samples; however, noble gas signatures are not anomalous, suggesting that if oil-field water is the source of BTEX, its fraction is much smaller. The source of oil-field water in these samples may be anthropogenic (leaky wells) or natural (faults and natural flowpaths). Large air-derived noble gas excesses from rapid recharge are apparent in Fruitvale Oil Field samples, whereas Lost Hills and South Belridge Oil Field samples are typically in the predicted equilibrium solubility range expected from natural distributed recharge. Anomalous excess air signatures trace rapid infiltration from the Kern River and managed enhanced recharge facilities. These results demonstrate the benefit of including noble gas analysis in the standard analytical procedure of investigating potential hydrocarbon gas sources in groundwater.

Declaration of Competing Interest

The authors declare that they have no known competing financial interests or personal relationships that could have appeared to influence the work reported in this paper.

Acknowledgements

This work was supported by the U.S. Geological Survey as part of the California State Water Resources Control Board's Oil and Gas Regional Monitoring Program. The complete data for this study are available in the USGS data releases (Davis et al., 2018; Dillion et al., 2016; Gannon et al., 2018; Gillespie et al., 2019; McCarlson et al., 2018). Any use of trade, firm, or product names is for description purposes only and does not imply endorsement by the U.S. Government.

Appendix A. Supplementary data

Supplementary data to this article can be found online at https://doi.org/10.1016/j.chemgeo.2021.120491.

References

Aeschbach-Hertig, W., El-Gamal, H., Wieser, M., Palcsu, L., 2008. Modeling excess air and degassing in groundwater by equilibrium partitioning with a gas phase. Water Resour. Res. 44, 1–12. https://doi.org/10.1029/2007WR006454.

Ballentine, C.J., Hall, C.M., 1999. Determining paleotemperature and other variables by using an error-weighted, nonlinear inversion of noble gas concentrations in water. Geochim. Cosmochim. Acta 63, 2315–2336. https://doi.org/10.1016/S0016-7037(99)00131-3.

Ballentine, C.J., O'Nions, R.K., Oxburgh, E.R., Horvath, F., Deak, J., 1991. Rare gas constraints on hydrocarbon accumulation, crustal degassing and groundwater flow in the Pannonian Basin. Earth Planet. Sci. Lett. 105, 229–246. https://doi.org/10.1016/0012-821X(91)90133-3.

Ballentine, C.J., O'Nions, R.K., Coleman, M.L., 1996. A Magnus opus: Helium, neon, and argon isotopes in a North Sea oilfield. Geochim. Cosmochim. Acta 60, 831–848. https://doi.org/10.1016/0016-7037(95)00439-4.

Ballentine, C.J., Burgess, R., Marty, B., 2002. Tracing fluid origin. Transport and Interaction in the Crust. Rev. Mineral. Geochemistry 47, 539–614. https://doi.org/10.2138/rmg.2002.47.13.

Barry, P.H., Lawson, M., Meurer, W.P., Warr, O., Mabry, J.C., Byrne, D.J., Ballentine, C. J., 2016. Noble gases solubility models of hydrocarbon charge mechanism in the Sleipner Vest gas field. Geochim. Cosmochim. Acta 194, 291–309. https://doi.org/10.1016/j.gca.2016.08.021.

Barry, P.H., Kulongoski, J.T., Landon, M.K., Tyne, R.L., Gillespie, J.M., Stephens, M.J., Hillegonds, D.J., Byrne, D.J., Ballentine, C.J., 2018. Tracing enhanced oil recovery signatures in casing gases from the lost Hills oil field using noble gases. Earth Planet. Sci. Lett. 496, 57–67. https://doi.org/10.1016/J.EPSL.2018.05.028.

Bosch, A., Mazor, E., 1988. Natural gas association with water and oil as depicted by atmospheric noble gases: case studies from the southeastern Mediterranean Coastal Plain. Earth Planet. Sci. Lett. 87, 338–346. https://doi.org/10.1016/0012-821X(88)90021-0.

Byrne, D.J., Barry, P.H., Lawson, M., Ballentine, C.J., 2018. Determining gas expulsion vs retention during hydrocarbon generation in the Eagle Ford Shale using noble gases. Geochim. Cosmochim. Acta 241, 240–254. https://doi.org/10.1016/j.gca.2018.08.042.

Byrne, D.J., Barry, P.H., Lawson, M., Ballentine, C.J., 2020. The use of noble gas isotopes to constrain subsurface fluid flow and hydrocarbon migration in the East Texas Basin. Geochim. Cosmochim. Acta 268, 186–208.

CalGEM, 2020. Oil and Gas Online Data, California Department of Conservation, Geologic Energy Management Division [WWW Document]. URL. https://www.conservation.ca.gov/calgem/Online_Data/Pages/Index.aspx.

California Department of Conservation, 1998. California Oil & Gas Fields. Division of Oil, Gas, and Geothermal Resources, Volume 1–Central California.

Cey, B.D., Hudson, G.B., Moran, J.E., Scanlon, B.R., 2008. Impact of Artificial Recharge on Dissolved Noble gases in Groundwater in California. Environ. Sci. Technol. 42, 1017–1023. https://doi.org/10.1021/es0706044.

Crovetto, R., Fernández-Prini, R., Japas, M.L., 1982. Solubilities of inert gases and methane in H_2O and in D_2O in the temperature range of 300 to 600 K. J. Chem. Phys. 76, 1077–1086. https://doi.org/10.1063/1.443074.

CSWRCB, 2019. Water Quality in Areas of Oil and Gas Production – Regional Groundwater Monitoring [WWW Document]. URL. https://www.waterboards.ca.gov/water_issues/programs/groundwater/sb4/regional_monitoring/.

Darrah, T.H., Vengosh, A., Jackson, R.B., Warner, N.R., Poreda, R.J., 2014. Noble gases identify the mechanisms of fugitive gas contamination in drinking-water wells overlying the Marcellus and Barnett Shales. Proc. Natl. Acad. Sci. 111, 14076–14081. https://doi.org/10.1073/pnas.1322107111.

Darrah, T.H., Jackson, R.B., Vengosh, A., Warner, N.R., Whyte, C.J., Walsh, T.B., Kondash, A.J., Poreda, R.J., 2015. The evolution of Devonian hydrocarbon gases in shallow aquifers of the northern Appalachian Basin: Insights from integrating noble gas and hydrocarbon geochemistry. Geochim. Cosmochim. Acta 170, 321–355. https://doi.org/10.1016/j.gca.2015.09.006.

Davis, T., Landon, M.K., Bennett, G.L., 2018a. Prioritization of Oil and Gas Fields for Regional Groundwater Monitoring Based on a Preliminary Assessment of Petroleum Resource Development and Proximity to California's Groundwater Resources Report 2018–5065. US Geological Survey. https://doi.org/10.3133/sir20185065.

Davis, T.A., Teunis, J.A., McCarlson, A.A., Seitz, N.O., Johnson, J.C., 2018b. Water Chemistry Data for Samples Collected at Groundwater and Surface-Water Sites near the Lost Hills and Belridge Oil Fields, November 2016–September 2017, Kern County, California: U.S. Geological Survey, Data Release. https://doi.org/10.5066/F7NS0T5M.

Dillion, D.B., Davis, T.A., Landon, M.K., Land, M.T., Wright Michael, T., Kulongoski, J.T., 2016. Data from exploratory sampling of groundwater in selected oil and gas areas of coastal Los Angeles County and Kern and Kings Counties in southern San Joaquin Valley, 2014–15: California Oil, Gas, and Groundwater Project (ver. 1.1, October 2017). U.S. Geol. Surv. Open-File Rep. https://doi.org/10.3133/ofr20161181, 2016–1181 24.

Dusseault, M., Jackson, R., 2014. Seepage pathway assessment for natural gas to shallow groundwater during well stimulation, in production, and after abandonment. Environ. Geosci. 21, 107–126.

EPA US, 2009. National primary drinking water regulations. https://www.epa.gov/sites/default/files/2016-06/documents/npwdr_complete_table.pdf accessed 26/08/2021.

Etiope, G., Sherwood Lollar, B., 2013. Abiotic methane on Earth. Rev. Geophys. 51, 276–299. https://doi.org/10.1002/rog.20011.

Etiope, G., Feyzullayev, A., Baciu, C.L., 2009. Terrestrial methane seeps and mud volcanoes: a global perspective of gas origin. Mar. Pet. Geol. 26, 333–344.

Faunt, C., 2009. Groundwater availability of the Central Valley aquifer, California. Groundw. Availab. Cent. Val. Aquifer, Calif. U.S. Geol. Surv. Prof. Pap. 1766, 225.

Frink, J.W., Kues, H.A., 1954. Corcoran Clay–a Pleistocene Lacustrine Deposit in San Joaquin Valley, California. Am. Assoc. Pet. Geol. Bull. 38, 2357–2371.

Füri, E., Hilton, D.R., Brown, K.M., Tryon, M.D., 2009. Helium systematics of cold seep fluids at Monterey Bay, California, USA: Temporal variations and mantle contributions. Geochemistry, Geophys. Geosystems 10. https://doi.org/10.1029/2009GC002557.

Gannon, R.S., Saraceno, J.F., Kulongoski, J.T., Teunis, J.A., Barry, P.H., Tyne, R.L., Kraus, T.E.C., Hansen, A.M., Qi, S.L., 2018. Produced water chemistry data for the lost Hills, Fruitvale, and North and south Belridge study areas, Southern San Joaquin Valley, California - ScienceBase-Catalog. https://doi.org/10.5066/F7X929H9.

Gillespie, J.M., Davis, T.A., Ball, L.B., Herrera, P.J., Wolpe, Z., Medrano, V., Bobbitt, M., Stephens, M.J., 2019a. Geological, geochemical, and geophysical data from the Lost Hills and Belridge oil fields (ver. 2.0, September 2019). https://doi.org/10.5066/P90QH6CI.

Gillespie, Janice M., Davis, T.A., Stephens, M.J., Ball, L.B., Landon, M.K., 2019b. Groundwater salinity and the effects of produced water disposal in the lost Hills–Belridge oil fields, Kern County, California. Environ. Geosci. 26, 73–96. https://doi.org/10.1306/eg.02271918009.

Gilman, J.B., Lerner, B.M., Kuster, W.C., De Gouw, J.A., 2013. Source signature of volatile organic compounds from oil and natural gas operations in northeastern Colorado. Environ. Sci. Technol. 47, 1297–1305. https://doi.org/10.1021/es304119a.

Graham, D.W., 2002. Noble Gas Isotope Geochemistry of Mid-Ocean Ridge and Ocean Island Basalts: Characterization of Mantle Source Reservoirs. Rev. Mineral. Geochemistry 47, 247–317. https://doi.org/10.2138/rmg.2002.47.8.

Gross, S.A., Avens, H.J., Banducci, A.M., Sahmel, J., Panko, J.M., Tvermoes, B.E., 2013. Analysis of BTEX groundwater concentrations from surface spills associated with hydraulic fracturing operations. J. Air Waste Manage. Assoc. 63, 424–432.

Harkness, J.S., Darrah, T.H., Warner, N.R., Whyte, C.J., Moore, M.T., Millot, R., Kloppmann, W., Jackson, R.B., Vengosh, A., 2017. The geochemistry of naturally occurring methane and saline groundwater in an area of unconventional shale gas development. Geochim. Cosmochim. Acta 208, 302–334. https://doi.org/10.1016/j.gca.2017.03.039.

Heilweil, V.M., Kip Solomon, D., Perkins, K.S., Ellett, K.M., 2004. Gas-partitioning tracer test to quantify trapped gas during recharge. Groundwater 42, 589–600.

Hluza, A.G., 1965. Summary of Operations, California oil Fields. California Department of Conservation, Division of Oil and Gas, vol. 51.

Hunt, A.G., 2015. U.S. Geological Survey Noble gas Laboratory's Standard Operating Procedures for the Measurement of Dissolved Gas in Water Samples. Techniques and Methods 5-A11, in: U.S. Geological Survey Techniques and Methods, p. 22. https://doi.org/10.3133/tm5A11.

Jung, M., Aeschbach, W., 2018. A new software tool for the analysis of noble gas data sets from (ground)water. Environ. Model. Softw. 103, 120–130. https://doi.org/10.1016/j.envsoft.2018.02.004.

Karolytė, R., Johnson, G., Györe, D., Serno, S., Flude, S., Stuart, F.M., Chivas, A.R., Boyce, A., Gilfillan, S.M.V., 2019. Tracing the migration of mantle CO2 in gas fields and mineral water springs in south-East Australia using noble gas and stable isotopes. Geochim. Cosmochim. Acta 259, 109–128. https://doi.org/10.1016/j.gca.2019.06.002.

Kern County Water Agency, 2018. Improvement District no. 4 of the Kern County Water Agency.

Kharaka, Y.K., Specht, D.J., 1988. The solubility of noble gases in crude oil at 25–100 C. Appl. Geochem. 3, 137–144.

Kipfer, R., Aeschbach-Hertig, W., Peeters, F., Stute, M., 2002. Noble gases in Lakes and Ground Waters. Rev. Mineral. Geochem. 47, 615–700. https://doi.org/10.2138/rmg.2002.47.14.

Kulongoski, J.T., Hilton, D.R., Barry, P.H., Esser, B.K., Hillegonds, D., Belitz, K., 2013. Volatile fluxes through the big Bend section of the San Andreas Fault, California: Helium and carbon-dioxide systematics. Chem. Geol. 339, 92–102. https://doi.org/10.1016/j.chemgeo.2012.09.007.

Land, P.E., 1984. Lost Hills Oil Field. Pub. No. TR32, California Department of Conservation Division of Oil, Gas, and Geothermal Resources, Sacramento, CA, pp. 3–17.

Landon, M.K., Belitz, K., 2012. Geogenic sources of benzene in aquifers used for public supply, California. Environ. Sci. Technol. 46, 8689–8697.

Magoon, L.B., Lillis, P.G., Peters, K.E., 2009. Petroleum Systems Used to Determine the Assessment Units in the San Joaquin Basin Province, California. Pet. Syst. Geol. Assess. oil gas San Joaquin Basin Prov. Calif. US Geol. Surv. Prof. Pap.

Martini, A.M., Budal, J.M., Walter, L.M., Schoell, M., 1996. Microbial generation of economic accumulations of methane within a shallow organic-rich shale. Nature 383, 155–158. https://doi.org/10.1038/383155a0.

Martini, A.M., Walter, L.M., Budat, J.M., Ku, T.C.W., Kaiser, C.J., Schoell, M., 1998. Genetic and temporal relations between formation waters and biogenic methane: Upper Devonian Antrim shale, Michigan Basin, USA. Geochim. Cosmochim. Acta 62, 1699–1720. https://doi.org/10.1016/S0016-7037(98)00090-8.

Martini, A.M., Walter, L.M., Ku, T.C.W., Budai, J.M., McIntosh, J.C., Schoell, M., 2003. Microbial production and modification of gases in sedimentary basins: a

geochemical case study from a Devonian shale gas play, Michigan basin. Am. Assoc. Pet. Geol. Bull. 87, 1355–1375. https://doi.org/10.1306/031903200184.
McCarlson, A.A., Wright, M.T., Teunis, J.A., Davis, T.A., Johnson, J.C., Qi, S.L., 2018. Water chemistry data for samples collected at groundwater sites near the Fruitvale oil field, September 2016–February 2017, Kern County, California, U.S. Geological Survey, data release. https://doi.org/10.5066/F7ZW1K7T.
McIntosh, J.C., Hendry, M.J., Ballentine, C., Haszeldine, R.S., Mayer, B., Etiope, G., Elsner, M., Darrah, T.H., Prinzhofer, A., Osborn, S., Stalker, L., Kuloyo, O., Lu, Z.-T., Martini, A., Lollar, B.S., 2019. A critical Review of State-of-the-Art and Emerging Approaches to Identify Fracking-Derived gases and Associated Contaminants in Aquifers. Environ. Sci. Technol. 53, 1063–1077. https://doi.org/10.1021/acs.est.8b05807.
McMahon, P.B., Barlow, J.R.B., Engle, M.A., Belitz, K., Ging, P.B., Hunt, A.G., Jurgens, B. C., Kharaka, Y.K., Tollett, R.W., Kresse, T.M., 2017. Methane and benzene in drinking-water wells overlying the Eagle Ford, Fayetteville, and Haynesville Shale hydrocarbon production areas. Environ. Sci. Technol. 51, 6727–6734.
McMahon, P.B., Kulongoski, J.T., Vengosh, A., Cozzarelli, I.M., Landon, M.K., Kharaka, Y.K., Gillespie, J.M., Davis, T.A., 2018. Regional patterns in the geochemistry of oil-field water, southern San Joaquin Valley, California, USA. Appl. Geochemistry 98, 127–140. https://doi.org/10.1016/J.APGEOCHEM.2018.09.015.
McMahon, P.B., Vengosh, A., Davis, T.A., Landon, M.K., Tyne, R.L., Wright, M.T., Kulongoski, J.T., Hunt, A.G., Barry, P.H., Kondash, A.J., Wang, Z., Ballentine, C.J., 2019. Occurrence and sources of Radium in Groundwater Associated with Oil Fields in the Southern San Joaquin Valley, California. Environ. Sci. Technol. 53, 9398–9406. https://doi.org/10.1021/acs.est.9b02395.
Miller, R.H., Bloom, C.V., 1939. Mountain View Oil Field, in California Department of Conservation, Oil and Gas Annual Reports, Summary of Operations.
Mount, J., Hanak, E., 2014. Water Use in California. Public Policy Inst. Calif.
Njobuenwu, D.O., Amadi, S.A., Ukpaka, P.C., 2005. Dissolution rate of BTEX contaminants in water. Can. J. Chem. Eng. 83, 985–989.
O'Nions, R.K., Oxburgh, E.R., 1988. Helium, volatile fluxes and the development of continental crust. Earth Planet. Sci. Lett. 90, 331–347. https://doi.org/10.1016/0012-821X(88)90134-3.
Ozima, M., Podosek, F.A., 2002. Noble Gas Geochemistry. Cambridge University Press. https://doi.org/10.1017/CBO9781107415324.004
Prinzhofer, A., 2013. Noble Gases in Oil and Gas Accumulations, in: The Noble Gases as Geochemical Tracers. Springer, Berlin Heidelberg, Berlin, Heidelberg, pp. 225–247. https://doi.org/10.1007/978-3-642-28836-4_9.
Scheirer, A.H., Magoon, L.B., 2007. Age, distribution, and stratigraphic relationship of rock units in the San Joaquin Basin province, California, Petroleum systems and geologic assessment of oil and gas in the San Joaquin Basin province, California: US Geologic Survey Professional Paper. https://doi.org/10.3133/pp1713.
Shores, A., Laituri, M., Butters, G., 2017. Produced water surface spills and the risk for BTEX and naphthalene groundwater contamination. Water Air Soil Pollut. 228, 1–13.
Smith, S.P., Kennedy, B.M., 1983. The Solubility of Noble Gases in Water and in NaCl Brine*. Pcrgamon Press Lid.
Stute, M., Deak, J., 1989. Environmental Isotope Study (14C, 13C, 18O, D, Noble gases) on Deep Groundwater Circulation Systems in Hungary with Reference to Paleoclimate. Radiocarbon 31, 902–918. https://doi.org/10.1017/S0033822200012522.
Tyne, R.L., Barry, P.H., Hillegonds, D.J., Hunt, A.G., Kulongoski, J.T., Stephens, M.J., Byrne, D.J., Ballentine, C.J., 2019. A Novel Method for the Extraction, Purification, and Characterization of Noble Gases in Produced Fluids. Geochemistry, Geophys. Geosystems. https://doi.org/10.1029/2019GC008552, 2019GC008552.
USGS, 2020. California Oil, Gas, and Groundwater (COGG) Program [WWW Document] URL. https://ca.water.usgs.gov/projects/oil-gas-groundwater/.
Wen, T., Castro, M.C., Nicot, J.P., Hall, C.M., Larson, T., Mickler, P., Darvari, R., 2016. Methane sources and Migration Mechanisms in Shallow Groundwaters in Parker and Hood Counties, Texas - a Heavy Noble Gas Analysis. Environ. Sci. Technol. 50, 12012–12021. https://doi.org/10.1021/acs.est.6b01494.
Wen, T., Castro, M.C., Nicot, J.P., Hall, C.M., Pinti, D.L., Mickler, P., Darvari, R., Larson, T., 2017. Characterizing the Noble Gas Isotopic Composition of the Barnett Shale and Strawn Group and Constraining the source of Stray Gas in the Trinity Aquifer, North-Central Texas. Environ. Sci. Technol. 51, 6533–6541. https://doi.org/10.1021/acs.est.6b06447.
Whiticar, M.J., 1999. Carbon and hydrogen isotope systematics of bacterial formation and oxidation of methane. Chem. Geol. 161, 291–314. https://doi.org/10.1016/S0009-2541(99)00092-3.
Wilde, F.D., 2010. Water-quality sampling by the US Geological Survey: standard protocols and procedures. US Geol. Surv. Fact Sheet 312.
Wright, M.T., McMahon, P.B., Landon, M.K., Kulongoski, J.T., 2019. Groundwater quality of a public supply aquifer in proximity to oil development, Fruitvale oil field, Bakersfield, California. Appl. Geochemistry 106, 82–95. https://doi.org/10.1016/J.APGEOCHEM.2019.05.003.